Proc. Natl. Acad. Sci. USA
Vol. 90, pp. 3202–3206, April 1993
Microbiology

Calcium influx mediated by the *Escherichia coli* heat-stable enterotoxin B (ST_B)

LAWRENCE A. DREYFUS*†, BETH HARVILLE*, DANIEL E. HOWARD‡, RADWAN SHABAN*, DIANE M. BEATTY*, AND STEPHEN J. MORRIS‡

Divisions of *Cell Biology and Biophysics and ‡Molecular Biology and Biochemistry, University of Missouri, Kansas City, MO 64110-2499

Communicated by Harley W. Moon, December 31, 1992 (received for review November 18, 1992)

ABSTRACT **The heat-stable enterotoxin B (ST_B) of *Escherichia coli* is a 48-amino acid extracellular peptide that induces rapid fluid accumulation in animal intestinal models. Unlike other *E. coli* enterotoxins that elicit cAMP or cGMP responses in the gut [heat-labile toxin (LT) and heat-stable toxin A (ST_A), respectively], ST_B induces fluid loss by an undefined mechanism that is independent of cyclic nucleotide elevation. Here we studied the effects of ST_B on intracellular calcium concentration ($[Ca^{2+}]_i$), another known mediator of intestinal ion and fluid movement. Ca^{2+} and pH measurements were performed on different cell types including Madin–Darby canine kidney (MDCK), HT-29/C_1 intestinal epithelial cells, and primary rat pituitary cells. Ca^{2+} and pH determinations were performed by simultaneous real-time fluorescence imaging at four emission wavelengths. This allowed dual imaging of the Ca^{2+}- and pH-specific ratio dyes (indo-1 and SNARF-1, respectively). ST_B treatment induced a dose-dependent increase in $[Ca^{2+}]_i$ with virtually no effect on internal pH in all of the cell types tested. ST_B-mediated $[Ca^{2+}]_i$ elevation was not inhibited by drugs that block voltage-gated Ca^{2+} channels including nitrendipine, verapamil (L-type), ω-conotoxin (N-type), and Ni^{2+} (T-type). The increase in $[Ca^{2+}]_i$ was dependent on a source of extracellular Ca^{2+} and was not affected by prior treatment of MDCK cells with thapsigargin or cyclopiazonic acid, agents that deplete and block internal Ca^{2+} stores. In contrast to these results, somatostatin and pertussis toxin pretreatment of MDCK cells completely blocked the ST_B-induced increase in $[Ca^{2+}]_i$. Taken together, these data suggest that ST_B opens a GTP-binding regulatory protein-linked receptor-operated Ca^{2+} channel in the plasma membrane. The nature of the ST_B-sensitive Ca^{2+} channel is presently under investigation.**

Enterotoxigenic *Escherichia coli* cause diarrheal disease in man and animals by the production of protein or peptide toxins. Two classes of enterotoxins, separated on the basis of thermal stability, are recognized. Heat-labile enterotoxins (LTs) of *E. coli* (LT-I and LT-II) are multimeric proteins that share antigenic, structural, and mechanistic similarity with cholera toxin (1). In contrast, the *E. coli* heat-stable enterotoxins (STs) are peptides that induce rapid fluid secretion in animal gut loop models (2, 3) and bear no resemblance to cholera toxin or LTs (4, 5). Two *E. coli* heat-stable enterotoxins (ST_A and ST_B) are currently recognized. ST_A is an 18- (or 19)-amino acid cysteine-rich, heat- and protease-stable peptide (6–8) that elevates mucosal cGMP by stimulation of a particulate guanylate cyclase (9). After binding of the toxin to a unique intestinal receptor (10, 11), the subsequent rise in cGMP presumably results in a rapid increase in net chloride secretion. In contrast to ST_A, ST_B is a 48-amino acid basic peptide (5) that, although like ST_A is heat-stable and cysteine-rich, is sensitive to trypsin proteolysis and bears no apparent structural similarity to ST_A (5, 12). Previous work by Weikel *et al.* (13, 14) indicates that ST_B induces a rapid short-circuit current across porcine intestinal mucosa. Evidence for chloride transport was not observed, yet electrogenic anion secretion, possibly bicarbonate, was observed in the absence of elevated cyclic nucleotides (14, 15). Beyond these few studies, nothing is known of the mechanism of ST_B action.

Evidence that suggests a receptor-mediated mode of ST_B action includes short-circuit current responses when toxin is delivered to the mucosal, but not serosal, side of intestinal tissue mounted in Ussing chambers (13); a rapid ST_B response in experiments utilizing either mounted tissue or whole animal models (15 min and 2 hr, respectively) (13, 14, 16); and the lack of apparent damage to the intestinal mucosa following ST_B treatment (17, 18). Known mediators of membrane signal transduction include cAMP, cGMP, the phosphatidylinositol 4,5-bisphosphate-derived metabolites inositol 1,4,5-trisphosphate ($Ins P_3$) and diacyl glycerol, and Ca^{2+} (for reviews, see refs. 19–21). Since pathways for Ca^{2+}-mediated intestinal secretion are known (22) and cyclic nucleotides are apparently not involved in the toxicity of ST_B, we examined the effect of ST_B on the internal Ca^{2+} concentration ($[Ca^{2+}]_i$) of transformed and primary cells of different tissues and species of origin. Our results suggest that ST_B induces a rapid dose-dependent influx of extracellular Ca^{2+} in cells of intestinal and nonintestinal origin; this Ca^{2+} influx mediated by ST_B appears to occur through a pertussis toxin-sensitive, GTP-binding regulatory protein (G protein)-regulated Ca^{2+} channel.

EXPERIMENTAL PROCEDURES

Toxin Preparation. ST_B was purified by a modification of our recently reported method (5). Briefly, *E. coli* 1790 (provided by Shannon C. Whipp, U.S. Department of Agriculture–Agricultural Research Services National Animal Disease Center, Ames, IA) harboring pPD21K, a kanamycin-resistant derivative of a *tac*-promoted *estB* coding vector (23), was grown in 24 liters of M9 medium (5) containing glucose (0.2%) and kanamycin (50 μg/ml) (12 × 6-liter flasks, each containing 2 liters) for 18 hr at 37°C with vigorous aeration. After growth, bacterial cells were removed by ultrafiltration through a 0.1-μm hollow fiber cartridge mounted in an Amicon DC-10 preparative ultrafiltration device (Amicon). The filtrate was passed sequentially through spiral membrane cartridges of 100 kDa and 3 kDa exclusion to remove high molecular weight material and to concentrate the ST_B-containing fraction, respectively. The concentrated filtrate was fractionated by HPLC on a Waters 25 × 100 mm DeltaPak C_4 preparative column (Water Division, Millipore), followed by Mono-S cation-exchange fast protein liquid chromatography (FPLC)

The publication costs of this article were defrayed in part by page charge payment. This article must therefore be hereby marked "*advertisement*" in accordance with 18 U.S.C. §1734 solely to indicate this fact.

Abbreviations: ST, heat-stable enterotoxin; $[Ca^{2+}]_i$, intracellular Ca^{2+} concentration; MDCK, Madin–Darby canine kidney; G protein, GTP-binding regulatory protein; LT, heat-labile enterotoxin; $Ins P_3$, inositol 1,4,5-trisphosphate; CPA, cyclopiazonic acid.

†To whom reprint requests should be addressed.

(Pharmacia Biotechnology). Finally, the toxin preparation was subjected to reverse-phase FPLC over a PepRPC 15 column (unpublished data). The ST_B preparation was judged pure by each of the following criteria: SDS/PAGE analysis followed by silver staining, amino acid composition analysis, and automated Edman degradation as described (5).

Cells and Cell Lines. Madin–Darby canine kidney (MDCK) cells (24), obtained as an outgrown secretory cell line from J. Grantham (University of Kansas Medical Center, Kansas City), were grown at 37°C in an atmosphere of 95% air/5% CO_2. Growth medium consisted of Dulbecco's modified Eagle's medium (DMEM; Sigma) supplemented with 10% (vol/vol) fetal bovine serum (FBS; JRH Scientific, Lenexa, KS), penicillin (100 units/ml), and streptomycin (100 μg/ml). HT-29/C_1 intestinal epithelial cells (25) were obtained from Cynthia L. Sears (The Johns Hopkins University School of Medicine, Baltimore) and grown in an atmosphere of 90% air/10% CO_2. Growth medium was DMEM (Sigma) supplemented with 10% FBS, 1 mM pyruvate, 44 mM $NaHCO_3$, human transferrin (10 μg/ml; GIBCO/BRL), penicillin (100 units/ml), and streptomycin (100 μg/ml).

Primary pituitary intermediate lobe melanotropes were isolated as follows (26): male Sprague–Dawley rats (150–175 g; Sasco, Omaha, NE) were anesthetized by i.p. injection with Nembutal (200 mg/kg; Abbott) and sacrificed by decapitation; after exposure of the brain, the neurointermediate lobe was dissected from the anterior lobe, and lobules from one intermediate lobe were teased from the neural lobe and divided among 6 wells of a 12-well tissue culture plate, each containing a no. 00 coverslip (Corning) coated with poly(L-lysine) (Sigma). The cells were grown in CellGro Plus medium (Fisher Scientific) supplemented with 5% FBS, penicillin (100 units/ml), and streptomycin (100 μg/ml) in an atmosphere of 93% air/7% CO_2. The explants were allowed to grow until the lobules were well attached to the coverslips and a confluent monolayer of cells surrounded the explant (10–14 days).

Loading Cells with Fluorescent Dyes. MDCK and HT-29/C_1 cells were stripped from culture flasks by treatment with 0.01% trypsin/0.05 mM EDTA (JRH Scientific) when culture flasks reached 75–80% confluence. Cells were washed free of trypsin/EDTA, and 1×10^5 to 5×10^5 cells were seeded onto sterile no. 00 coverslips, which were flooded with complete medium (see above) and incubated as described above. Cells plated on coverslips 2–3 days prior to experiments were simultaneously loaded with 5 μM indo-1,AM and 5 μM SNARF-1,AM, both cell-permeant acetoxymethyl (AM) esters (Molecular Probes), in DMEM (Sigma) containing 0.02% Pluronic F-127 detergent (Molecular Probes) and 12.5% (vol/vol) dimethyl sulfoxide for 30 min at 37°C in an atmosphere of 93% air/7% CO_2. After the incubation period, cells were washed with DMEM and maintained in 93% air/7% CO_2 at 37°C in DMEM supplemented with 5% FBS for a 1-hr recovery period to allow esterase cleavage of the dyes to the impermeable form. Cells were used within 90 min of this recovery period. Labeling of intermediate lobe pituitary cells was performed as just described for MDCK and HT-29/C_1 cells.

Ca^{2+} and pH Measurements. Dye-loaded cells on coverslips were placed in 1.0 ml of standard balanced salt solution (BSS) (138 mM NaCl/2 mM KCl/2 mM $MgCl_2$/5.5 mM glucose/50 μM EGTA/10 mM Hepes, pH 7.4) contained in a microscope-stage perfusion chamber maintained at 37°C. For the standard assay, 10 μl of toxin solution was added to the bath (final toxin concentration, 500 nM). Two to four minutes after the addition of toxin, $CaCl_2$ was added to a final concentration of 3 mM. For other experiments, the addition time of drugs or ST_B or both was varied as noted. Additions of toxin, drugs, and Ca^{2+} were made directly to the perfusion chamber from 10–100× concentrated solutions made either in BSS or organic solvents as in the case of some of the drugs used (see below).

Simultaneous Ca^{2+} and pH measurements were made on a new design of a multiimaging fluorescence videomicroscope, which has been described in detail (27). By monitoring four emission wavelengths, the microscope performs simultaneous real-time capture of four separate fluorescence emission images. The fluorescent dyes were excited at 350 nm (indo-1) and 540 nm (SNARF-1) and imaged at 405, 475, 575, and 640 nm. Each emission wavelength was imaged simultaneously by one of four cameras at standard video-frame rates and then stored on 3/4″ video tape for further off-line analysis by digital image processing (describer below). The pH maps generated by this analysis were used to correct the Ca^{2+} maps for the pH dependence of indo-1. The integrated Ca^{2+} and pH values for 5–20 cells were extracted from the video data and transferred directly to SigmaPlot 4.1 (Jandel, Corte Madera, CA) for plotting; representative responses of cells were then graphed. Ca^{2+} standards were determined with free indo-1 and commercial Ca^{2+} buffers (Molecular Probes) at a series of defined free-Ca^{2+} concentrations between 0 (R_{min} below) and 40 μM. R_{max} (below) was taken as 40 mM $CaCl_2$. Standards for SNARF-1 were obtained at various pH values between 5.0 and 8.0 by using free SNARF-1 dye and pH-adjusted basic buffer. Experiments were repeated at least twice on at least two different days.

Analysis of Recorded Images. This has been discussed in detail (27). The dye–Ca^{2+} dissociation constant (K_d) of indo 1 and fura 2 is dependent upon prevailing pH (28, 29). Rather than presuming that the intracellular pH remains fixed throughout the experiment, we used the recorded intracellular pH to calculate a corrected $[Ca^{2+}]_i$. The taped images were corrected for background, shading error, and spillover of indo fluorescence into the SNARF images. For each cell, the integrated fluorescence from the 575- and 640-nm image was used to form a ratio value for calculation of pH by Eq. 1 (30):

$$pH = pKa + \log(Sf_2/Sb_2) + \log[(R - R_{min})/(R_{max} - R)], \quad [1]$$

where R, R_{max}, and R_{min} are the actual, maximal, and minimal ratios of the SNARF data, (Sf_2/Sb_2) is the ratio of free and bound dye at the R denominator wavelength, and pKa = 7.30. This value was then used to calculate a pH-corrected value of K_d for indo 1:

$$K_{d_{corr}} = (K_{d_{max}} + 10^{(pH-pK_a)} \cdot K_{d_{min}})/(10^{(pH-pK_a)} + 1). \quad [2]$$

Values for $K_{d_{max}}$, $K_{d_{min}}$, and pKa at 37°C of 80.9 μM, 141 nM, and 3.65 were calculated from a least-squares fit of Eq. 2 to the data for indo/EGTA as published by Lattanzio (28, 29). The ratio of the 405-nm and 475-nm images and the corrected K_d were used to calculate the corrected Ca^{2+} value:

$$[Ca^{2+}]_i = K_{d_{corr}} \cdot (Sf_2/Sb_2) \cdot [(R - R_{min})/(R_{max} - R)], \quad [3]$$

where R, R_{max}, and R_{min} are defined as above for the indo data.

Pharmacologic Agents. Thapsigargin, cyclopiazonic acid (CPA), pertussis toxin, somatostatin, verapamil, nitrendipine, and ω-conotoxin were obtained from Sigma. Thapsigargin, verapamil, and nitrendipine were dissolved in ethanol, CPA was dissolved in DMSO, and then all were diluted to their respective working concentration in BSS. The final concentration of solvent in the microscope stage bath was 1% ethanol when using thapsigargin and nitrendipine and was 1% dimethyl sulfoxide when using CPA. Control experiments using 1% ethanol and 1% dimethyl sulfoxide resulted in no effect on normal cell function or $[Ca^{2+}]_i$. All other agents were dissolved in BSS.

RESULTS

Effect of ST_B on $[Ca^{2+}]_i$. The addition of 3 mM Ca^{2+} to indo-1- and SNARF-1-preloaded cells had no effect on $[Ca^{2+}]_i$ or cellular pH; however, ST_B pretreatment (*ca.* 500 nM) of cells in Ca^{2+}-free medium resulted in a rapid increase in $[Ca^{2+}]_i$. Typical responses of MDCK and HT-29/C_1 cells to treatment with 50 nM ST_B are shown in Fig. 1. The response of melanotropes to ST_B (not shown) was similar to that of MDCK and HT-29/C_1. In the case of MDCK and melanotropes, no change in pH was observed over the course of ST_B action, whereas a slight decline in pH was observed after the addition of ST_B to HT-29/C_1 cells. Since all three cell types tested exhibited similar responses to ST_B, we selected the MDCK cell line to investigate further the effect of toxin on $[Ca^{2+}]_i$. ST_B treatment of MDCK cells resulted in a dose-dependent rise in $[Ca^{2+}]_i$ as shown in Table 1. $[Ca^{2+}]_i$ elevation ranged from a 2- to nearly 4-fold increase over resting levels, while internal pH was not significantly affected during the course of the experiments, even at the highest ST_B dose. This is in contrast to a number of secretory cell types, which show sharp decreases in pH_i when $[Ca^{2+}]_i$ is increased by influx through L-type Ca^{2+} channels. The duration of elevated $[Ca^{2+}]_i$ was also dose-dependent, lasting only 1–2 min with 50 nM ST_B and 5–6 min in higher doses (not shown), after which time $[Ca^{2+}]_i$ returned to the resting level (*ca.* 200 nM).

Table 1. Dose-dependent change in $[Ca^{2+}]_i$

ST_B dose,* nM	$\Delta[Ca^{2+}]_i$†
0	0
50	90.7 ± 23
500	239.9 ± 7.7
5000	397.8 ± 127.9

*ST_B dose is final concentration in microscope stage bath.
†Change in $[Ca^{2+}]_i$ is the difference between the concentration at the time of ST_B addition and the maximum response deflection.

Effect of ST_B on Internal Ca^{2+} Stores. In preliminary experiments we noted that the increase in $[Ca^{2+}]_i$ due to ST_B was not observed in the absence of extracellular Ca^{2+}. Therefore, we hypothesized that elevation of $[Ca^{2+}]_i$ was due to an influx of extracellular Ca^{2+} and not to release of Ca^{2+} from an internal store. To test this hypothesis, we treated MDCK cells with thapsigargin (31), a plant alkaloid that inhibits the sarcoplasmic reticulum Ca^{2+}-ATPase. Thapsigargin treatment induces release of $InsP_3$- and GTP-sensitive Ca^{2+} stores and inhibits their replenishment. Treatment of MDCK cells with thapsigargin did not diminish the ST_B-induced $[Ca^{2+}]_i$ rise; instead, thapsigargin-pretreatment sensitized MDCK cells to subsequent ST_B-mediated $[Ca^{2+}]_i$ elevation (Fig. 2). The enhancement of Ca^{2+} influx after treatment with thapsigargin has been observed in intermediate lobe melanotropes (D.M.B., unpublished data) and PC12 phaeochromocytoma cells (E. W. Westhead, personal communication). Depletion of intracellular Ca^{2+} stores by thapsigargin is known to activate ligand-gated plasma membrane Ca^{2+} channels (32). Identical results were seen in MDCK cells and melanotropes when internal Ca^{2+} stores were blocked with CPA, another Ca^{2+}-ATPase drug possessing similar activity to that of thapsigargin (33).

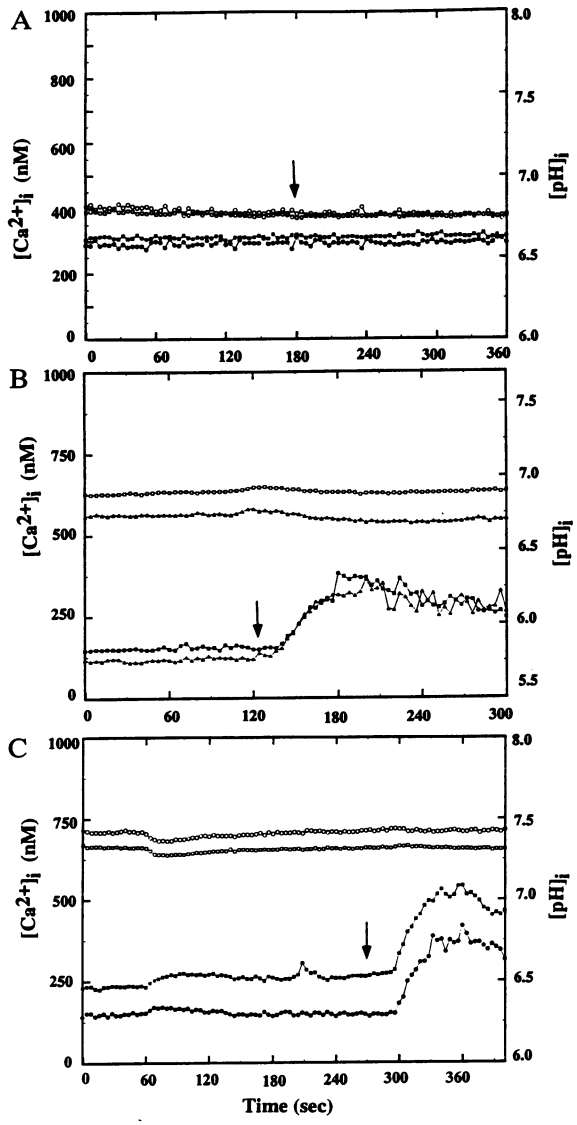

FIG. 1. Increase of $[Ca^{2+}]_i$ in response to ST_B. Timed measurements of $[Ca^{2+}]_i$ (closed symbols) and pH (open symbols) of individual control MDCK cells (*A*) or experimental MDCK cells (*B*) and HT-29/C_1 cells (*C*) treated with 500 nM ST_B. Cells were incubated in low Ca^{2+}-containing medium and treated (or not) with toxin 2–4 min prior to the addition of 3 mM Ca^{2+}. The arrow indicates the time of Ca^{2+} addition. Each pair of symbols (i.e., closed and open circles or closed and open triangles, etc.) represents determinations from a single cell; thus, each panel contains data from two cells.

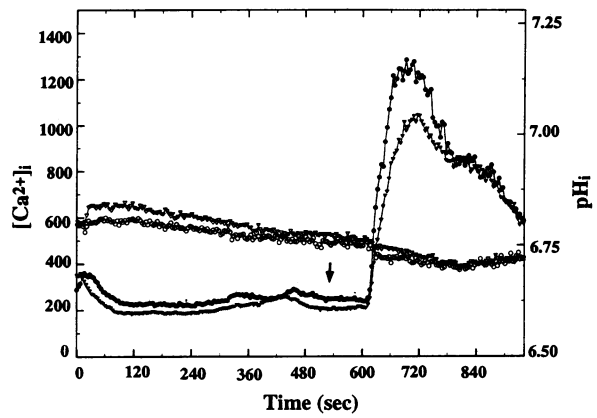

FIG. 2. Effect of thapsigargin treatment on ST_B-mediated $[Ca^{2+}]_i$ increase in MDCK cells. MDCK cells were treated with 300 nM thapsigargin for 2 hr prior to loading the cells with SNARF-1 and indo-1. Dye-loaded cells were placed in the microscope chamber and treated with 500 nM ST_B 4 min prior to the addition of Ca^{2+}, which is noted by the arrow. Closed symbols represent individual-cell $[Ca^{2+}]_i$; open symbols represent intracellular pH of the corresponding cells.

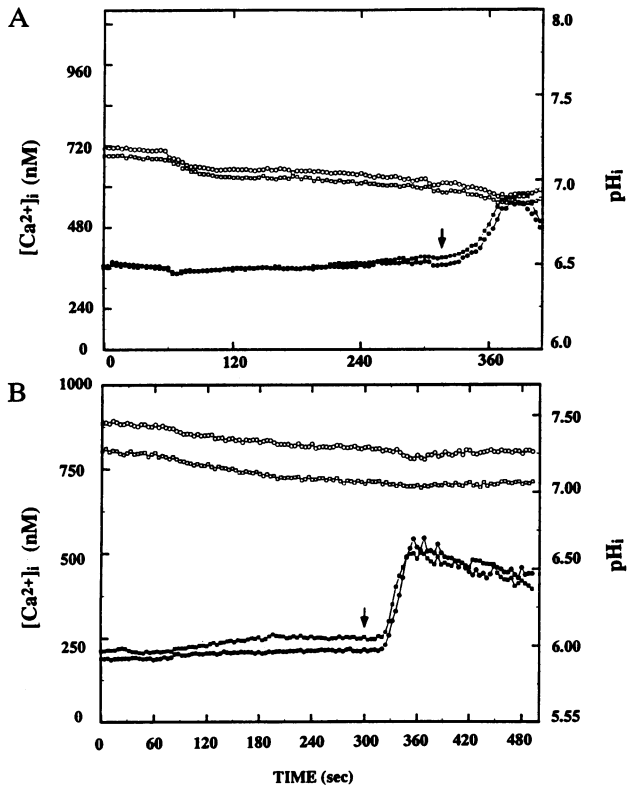

FIG. 3. Effect of Ca^{2+} channel blocking agents on ST_B-mediated Ca^{2+} increase in MDCK cells. MDCK cells were treated with 500 nM ST_B in the presence of 10 μM nitrendipine (*A*) and 40 μM nickel (*B*). Ca^{2+} addition is noted by the arrow in each panel. Closed symbols represent individual-cell $[Ca^{2+}]_i$; open symbols represent intracellular pH of the corresponding cells.

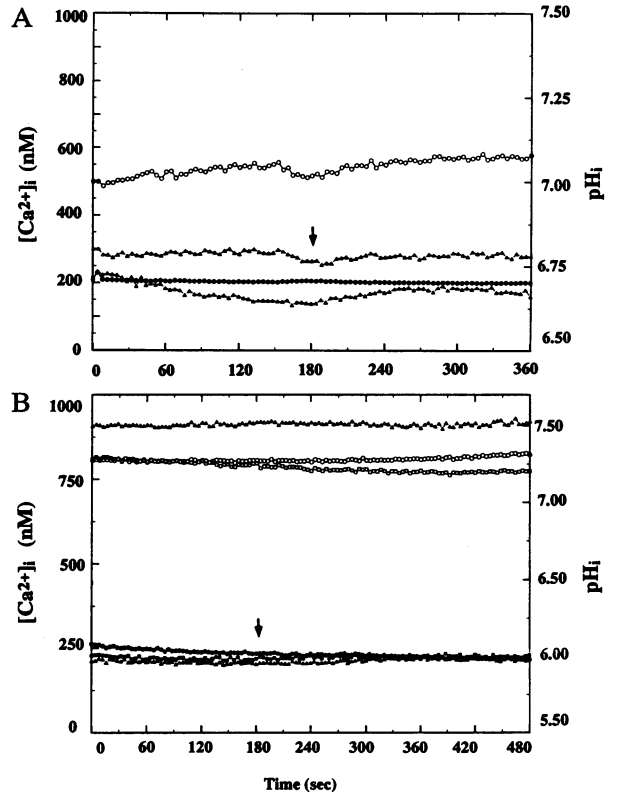

FIG. 4. Effect of somatostatin and pertussis toxin on ST_B-mediated Ca^{2+} increase in MDCK cells. Somatostatin (1 μM) was added to the cell bath 5 min prior to treatment of MDCK cells with 500 nM ST_B (*A*). Ca^{2+} was added as indicated by the arrow. MDCK cells were pretreated on coverslips for 2 hr with pertussis toxin at 1 μg/ml (*B*), rinsed, and loaded with fluorescent dyes as described. ST_B treatment (50 nM) preceded the addition of Ca^{2+} (as noted by the arrow) by 2 min. Closed symbols represent $[Ca^{2+}]_i$ levels of individual cells; open symbols represent intracellular pH of the corresponding cells.

Ca^{2+} Channel Blockers. The failure of ST_B to mediate release of Ca^{2+} from internal stores suggested that elevated $[Ca^{2+}]_i$ was a function of the opening of a plasma membrane Ca^{2+} channel. Elevation of MDCK cell $[Ca^{2+}]_i$ by ST_B treatment, however, was not blocked when the cell bath also contained 10 μM nitrendipine (Fig. 3*A*) or 10 μM verapamil (not shown), drugs that block L-type voltage-gated Ca^{2+} channels (34, 35). Similarly, 40 μM Ni^{2+}, an inhibitor of T-type voltage-gated Ca^{2+} channels (34), was also without effect on ST_B-induced Ca^{2+} elevation (Fig. 3*B*). Blockage of N-type Ca^{2+} channels by ω-conotoxin also failed to diminish the ST_B effect on MDCK cells (data not shown).

Role of G Proteins in ST_B-Mediated Ca^{2+} Entry. In contrast to these results, elevation of $[Ca^{2+}]_i$ in ST_B-treated MDCK cells was completely inhibited by pretreatment with 1 μM somatostatin and pertussis toxin at 1 μg/ml (Fig. 4). Taken together, these results suggest that ST_B induces an influx of extracellular Ca^{2+} through a receptor-operated (ligand-gated) Ca^{2+} channel on the plasma membrane of MDCK cells. The ST_B-responsive Ca^{2+} channel is apparently opened through the action of a PT-sensitive G protein.

DISCUSSION

This communication reports a biochemical action for the *E. coli* ST_B enterotoxin. Previous attempts to identify secondary messengers of ST_B action proved that the toxin exerts its biological effect without apparent elevations in cAMP or cGMP, hallmark activities of other *E. coli* enterotoxins. It is assumed that ST_B alters fluid and electrolyte transport in the gut after interaction with a mucosal receptor. Although the notion of a ST_B receptor is based on inference from Ussing chamber studies and *in vivo* models, this report strengthens the argument that a ST_B receptor exists; further, the receptor is present on cell types of both intestinal and nonintestinal origin.

Initial experiments investigating $[Ca^{2+}]_i$ of MDCK cells treated with ST_B indicated that little effect was observed when cells were bathed in high Ca^{2+}-containing buffer (3 mM). In contrast, we observed dramatic increases in $[Ca^{2+}]_i$ when cells were first incubated with toxin in Ca^{2+}-free medium or low calcium (0.5 or 1 mM)-containing medium before the extracellular Ca^{2+} concentration was raised to 3 mM. Increase of cellular $[Ca^{2+}]_i$ was not observed in the absence of toxin treatment. The results suggest that Ca^{2+} may influence the biochemical action of the toxin in such a way that binding of ST_B leading to activation of a Ca^{2+} channel occurs only under conditions of low extracellular Ca^{2+}. The high concentration of positive charge on ST_B (pI > 9.0) could, at the very least, promote ST_B association with the negatively charged polar head groups of the plasma membrane surface; in addition, the highly flexible and positively charged disulfide-bonded loop formed by ST_B residues 21–36 (Cys-Lys-Lys-Gly-Phe-Leu-Gly-Val-Arg-Asp-Gly-Thr-Ala-Gly-Ala-Cys) (5) could potentially compete for Ca^{2+}-binding sites at a channel or channel regulatory site. The 21–36 residue loop, and in particular residues Arg-29 (codon 53) and Asp-30 (codon 54), is known to be required for full expression of toxicity (5). The association of ST_B with plasma membrane is not known at this point.

The requirement for ST_B action in low Ca^{2+}-containing medium and sensitivity to somatostatin are similar to the

extracellular Ca^{2+}-mediated elevation of $[Ca^{2+}]_i$, and the concomitant release of calcitonin in calcitonin-secreting cells (C-cells) (36). Ca^{2+} influx in C-cells is mediated by a pertussis toxin-insensitive voltage-gated Ca^{2+} channel. In contrast, the action of ST_B is completely inhibited by pertussis toxin, indicating the role of a pertussis toxin-sensitive G protein [inhibitory (G_i) or "other" (G_o) G protein]. Known mechanisms of Ca^{2+} channel regulation by G proteins involve either stimulation by G_s (stimulatory G protein) subunits or inhibition through G_o activity (37). The former class is represented by the dihydropyridine-sensitive cardiac sarcolemmal Ca^{2+} channel, which relies on G_s-protein action (38). The latter class of channels is exemplified by the γ-aminobutyric acid $GABA_B$ receptor, which inhibits voltage-gated Ca^{2+} currents through the action of a pertussis toxin-sensitive G_o protein (39). The inhibition of the ST_B-mediated $[Ca^{2+}]_i$ increase by pertussis toxin suggests the involvement of a G protein, either G_i or G_o; although that toxin also inactivates G_p (phospholipase stimulatory G protein) action (37), the involvement of this G protein is unlikely, since we did not observe release of Ca^{2+} from an $InsP_3$-sensitive internal store. The argument for G-protein involvement in the ST_B-mediated increase in $[Ca^{2+}]_i$ is strengthened by the observed inhibitory effect of somatostatin, a G-protein antagonist (40). The reported inhibitory effect of somatostatin on G_s is attributed to the drug-dependent dissociation of G_i into α and $\beta\gamma$ subunits. Excess $\beta\gamma$ is thought to inhibit dissociation of G_s (and presumably G_o) (40).

Recently, Hitotsubashi *et al.* (41) presented data indicating a role for prostaglandin E_2 (PGE_2) in ST_B-mediated fluid secretion in the mouse. Fluid accumulation peaked at 3 hr concomitant with an approximate 3-fold increase in the level of PGE_2. Secretion was significantly blocked by indomethacin pretreatment of mice. The time course of intestinal secretion and PGE_2 accumulation relative to that presented here for Ca^{2+} influx suggests that events at the plasma membrane that cause increased $[Ca^{2+}]_i$ may trigger subsequent events, including PGE_2 synthesis and intestinal secretion.

The work was supported by research grants from the National Institutes of Health (AI32736 to L.A.D. and GM44071 to S.J.M.) and the National Science Foundation (BN9211912 to S.J.M.).

1. Robertson, D. C., McDonel, J. C. & Dorner, F. (1985) *Pharmacol. Ther.* **28,** 303–339.
2. Dean, A. G., Ching, Y. C., Williams, R. G. & Harden, L. B. (1972) *J. Infect. Dis.* **125,** 407–411.
3. Burgess, M. N., Bywater, R. J., Cowley, C. M., Mullan, N. A. & Newsome, P. M. (1978) *Infect. Immun.* **21,** 526–531.
4. Kupersztoch, Y. M., Tachias, K., Moomaw, C. R., Dreyfus, L. A., Urban, R. G., Slaughter, C. & Whipp, S. C. (1990) *J. Bacteriol.* **172,** 2427–2432.
5. Dreyfus, L. A., Urban, R. G., Whipp, S. C., Slaughter, C., Tachias, K. & Kupersztoch, Y. M. (1992) *Mol. Microbiol.* **6,** 2397–2406.
6. Takao, T., Hitouji, T., Aimoto, S., Shimonishi, Y., Hara, S., Takeda, T., Takeda, Y. & Miwatani, T. (1983) *FEBS Lett.* **152,** 1–5.
7. Staples, S. J., Asher, S. E. & Giannella, R. A. (1980) *J. Biol. Chem.* **247,** 1106–1113.
8. Dreyfus, L. A., Frantz, J. C. & Robertson, D. C. (1983) *Infect. Immun.* **42,** 537–543.
9. Field, M. L., Graf, L. H., Laird, W. J. & Smith, P. L. (1978) *Proc. Natl. Acad. Sci. USA* **75,** 2800–2804.
10. Frantz, J. C., Jaso-Freidman, L. J. & Robertson, D. C. (1984) *Infect. Immun.* **43,** 622–630.
11. Giannella, R. A., Luttrell, M. & Thompson, M. (1983) *Am. J. Physiol.* **245,** 6492–6498.
12. Whipp, S. C. (1987) *Infect. Immun.* **55,** 2057–2060.
13. Weikel, C. S. & Guerrant, R. C. (1985) in *Microbial Toxins and Diarrheal Disease*, eds. Evered, R. & Whelan, J. (Pitman, London), pp. 94–115.
14. Weikel, C. S., Nellans, H. N. & Guerrant, R. L. (1986) *J. Infect. Dis.* **153,** 893–901.
15. Kennedy, D. J., Greenberg, R. N., Dunn, J. A., Abernathy, R., Ryerse, J. S. & Guerrant, R. L. (1984) *Infect. Immun.* **46,** 639–643.
16. Whipp, S. C. (1990) *Infect. Immun.* **58,** 930–934.
17. Rose, R., Whipp, S. C. & Moon, H. W. (1987) *Vet. Pathol.* **24,** 71–79.
18. Whipp, S. C., Moseley, S. L. & Moon, H. W. (1986) *Am. J. Vet. Res.* **47,** 615–618.
19. Schramm, M. & Selinger, Z. (1984) *Science* **225,** 1350–1356.
20. Chinkers, M. & Garbers, D. L. (1991) *Annu. Rev. Biochem.* **60,** 553–575.
21. Abdel-Latif, A. A. (1986) *Pharm. Rev.* **38,** 227–272.
22. Powell, D. W. & Fan, C. C. (1983) in *Intestinal Transport*, eds. Gilles-Baillien, M. & Gilles, R. (Springer, Berlin), pp. 215–226.
23. Urban, R. G., Pipper, E. M., Dreyfus, L. A. & Whipp, S. C. (1990) *J. Clin. Microbiol.* **28,** 2383–2388.
24. Misfeldt, D. S., Hamamoto, S. T. & Pitelka, D. R. (1976) *Proc. Natl. Acad. Sci. USA* **73,** 1212–1216.
25. Weikel, C. S., Grieco, F. D., Rueben, J., Myers, L. L. & Sack, R. B. (1992) *Infect. Immun.* **60,** 321–327.
26. Chronwall, B. M., Bishop, J. F. & Gehlert, D. R. (1988) *Peptides* **9,** 169–180.
27. Morris, S. (1993) in *Optical Microscopy*, eds. Herman, B. & Lemasters, J. J. (Academic, New York), pp. 177–212.
28. Lattanzio, F. A. (1990) *Biochem. Biophys. Res. Commun.* **171,** 102–108.
29. Lattanzio, F. A. & Bartchat, D. K. (1991) *Biochem. Biophys. Res. Commun.* **177,** 184–191.
30. Martinez-Zaguilan, R., Martinez, G. M., Latanzio, F. & Gillies, R. J. (1991) *Am. J. Physiol.* **260,** C297–C307.
31. Thastrup, O., Cullen, P. J., Drobak, B. K., Hanley, M. R. & Dawson, A. P. (1990) *Proc. Natl. Acad. Sci. USA* **87,** 2466–2470.
32. Takemura, H., Hughes, A. R., Thastrup, O. & Putney, J. W., Jr. (1989) *J. Biol. Chem.* **264,** 12266–12271.
33. Seideler, N., Jona, I., Vegh, M. & Martonosi, A. (1989) *J. Biol. Chem.* **264,** 17816–17823.
34. Seth, S. D. & Seth, S. (1991) *Indian J. Pharmacol.* **35,** 217–231.
35. Bean, B. P. (1984) *Proc. Natl. Acad. Sci. USA* **81,** 6388–6392.
36. Scherübl, H., Hescherler, J., Schultz, G., Kliemann, D., Zink, A., Ziegler, R. & Raue, F. (1992) *Cell. Signalling* **4,** 77–85.
37. Birnbaumer, L., Abramowitz, J. & Brown, A. M. (1990) *Biochim. Biophys. Acta* **1031,** 163–224.
38. Yatani, A., Imoto, Y., Codinas, J., Hamilton, S. L., Brown, A. M. & Birnbaumer, L. (1988) *J. Biol. Chem.* **263,** 8997–9895.
39. Holz, G. G., Rane, S. G. & Dunlap, K. (1986) *Nature (London)* **319,** 670–672.
40. Ransnäs, L. A., Liebler, D. & Insel, P. A. (1991) *Biochem. J.* **280,** 303–307.
41. Hitotsubashi, S., Fugii, Y., Yamanaka, H. & Okamoto, K. (1992) *Infect. Immun.* **60,** 4468–4474.